

Hybrid ferrohydrodynamic instability: Coexisting peak and labyrinthine patterns

Ching-Yao Chen,^{1,*} W.-K. Tsai,² and José A. Miranda^{3,†}

¹*Department of Mechanical Engineering, National Chiao Tung University, Hsinchu, Taiwan, Republic of China*

²*Department of Mechanical Engineering, National Yunlin University of Science and Technology, Yunlin, Taiwan, Republic of China*

³*Departamento de Física, LFTC, Universidade Federal de Pernambuco, Recife, Pernambuco 50670-901, Brazil*

(Received 17 March 2008; published 12 May 2008)

We present an experimental study of a different pattern-forming instability occurring when a ferrofluid droplet is immersed in a thin layer of a nonmagnetic fluid, and subjected to a uniform perpendicular magnetic field. The formation of intriguing interfacial structures is observed, and the development of a hybrid-type ferrohydrodynamic instability is verified, where peak and labyrinthine ferrofluid patterns coexist and share a coupled dynamic evolution. Based on our experimental findings we have identified the occurrence of three well defined regimes for the evolution of the miscible Rosensweig peak in which it first grows rapidly, and then gradually decays, to ultimately reimmerse into the surrounding nonmagnetic solvent layer. This unique scenario for the rise and fall of the Rosensweig peak implies the simultaneous emergence of peculiar labyrinthine structures induced by an outward radial flow within the thin nonmagnetic layer. A variety of possible morphologies is revealed (labyrinth, broken tentaclelike fingers, etc.), which result from the interplay between magnetic, diffusive, and convective effects. These free surface flow labyrinthine structures are contrasted to alternative interfacial designs obtained when the experimental system is spatially confined.

DOI: [10.1103/PhysRevE.77.056306](https://doi.org/10.1103/PhysRevE.77.056306)

PACS number(s): 47.54.-r, 47.65.Cb, 47.51.+a, 47.20.Ma

I. INTRODUCTION

The field of ferrofluid research is highly interdisciplinary, and during the last few decades has been provoking a number of interesting scientific and technological developments of relevance to areas of physics, chemistry, engineering, and even medicine [1–3]. Ferrofluids are colloidal suspensions of nanometer-sized magnetic particles suspended in a nonmagnetic carrier fluid. These magnetic fluids behave superparamagnetically and can easily be manipulated with external magnetic fields. A unique interplay between hydrodynamic and magnetic forces make ferrofluids a fascinating material to study a variety of interfacial instabilities and pattern-forming processes [4,5].

One celebrated example of pattern formation phenomenon in such magnetic fluids is the Rosensweig instability [6–8], in which an initially flat ferrofluid surface exhibits a three-dimensional (3D) stationary hexagonal array of peaks when a uniform magnetic field is applied normal to it. In fact, the electric counterpart of the Rosensweig instability has been examined by G. I. Taylor who investigated the mathematical structure of similar peak structures (the “Taylor cones”) appearing in dielectric drops subjected to uniform electric fields [9]. Another type of visually striking patterns is associated with the so-called labyrinthine instability [10,11], where highly branched structures are formed when a ferrofluid droplet is trapped in the effectively two-dimensional (2D) geometry of a Hele-Shaw cell under a perpendicular uniform magnetic field. Labyrinthine-type patterns have been shown to form in thin films of dielectric fluids [12], and also in very diverse two-phase systems ranging from growing vegetation in arid regions [13] through drainage of granular-fluid systems [14].

In the ordinary 3D Rosensweig instability, the thickness of the immiscible ferrofluid layer is typically of the order of centimeters, so that it is comparable to the wavelength of the unstable surface mode. However, some research groups [15–18] have also examined the development of Rosensweig peaks in extremely thin immiscible ferrofluid films, whose characteristic thickness is considerably smaller [$O(10-10^3)\mu\text{m}$]. Under such circumstances, an interesting film rupture process takes place, with the peaks breaking up into individual droplets that preserve the hexagonal symmetry of the traditional Rosensweig instability. Regarding the effectively 2D labyrinthine instability, an alternative variation has also been studied: although the large majority of the investigations deal with immiscible ferrofluids, there are some suggestive experimental [19,20] and theoretical [21–23] works which consider that the confined magnetic fluid is indeed miscible. In this case, interfacial tension is negligible and diffusive effects become very important in determining the shape of the resulting patterned structures.

Despite the rich physics and the great variety of situations explored both theoretically and experimentally in the study of the peak and labyrinthine instabilities in ferrofluids, they are commonly presented as two compelling, but disjointed physical phenomena. In this work, we experimentally investigate a situation in which a hybrid ferrohydrodynamic instability arises, where peak and labyrinth patterns coexist and evolve simultaneously. This is made possible thanks to a suitable combination of two key physical ingredients exploited in Refs. [15–22]: (i) the possibility of reducing the thickness of the ferrofluid layer, and (ii) the feasibility of exploring the miscible nature of the magnetic fluid sample with respect to the surrounding nonmagnetic liquid. Here we put these ingredients together in an entirely different perspective, and show that by appropriately combining them one can observe the concomitant emergence of both Rosensweig and labyrinthine instabilities in a single experimental

*chingyao@mail.nctu.edu.tw

†jme@df.ufpe.br

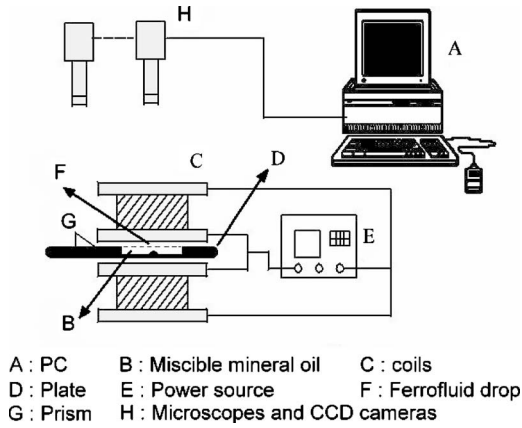


FIG. 1. Scheme of the experimental setup. See the text for details.

setup. As a result, appealing pattern morphologies and still unexplored dynamical behaviors are unveiled and discussed.

II. EXPERIMENTAL RESULTS AND DISCUSSION

A. Experimental setup

Figure 1 schematically sketches our experimental setup. We examine the time evolution of both the 3D peak and its coexisting effectively 2D diffusing interface when a droplet of ferrofluid is immersed in a thin layer of a miscible nonmagnetic fluid, and subjected to a perpendicular uniform magnetic field. Throughout this work, whenever we talk about a miscible “interface” we really mean the mixing region between the miscible fluids which is characterized by higher concentration gradients. Unlike the corresponding immiscible situation where a sharp interface separating the fluids can be well defined, the mixing region between miscible fluids is not a clear boundary, but rather a diffuse layer. However, in the regions of significant concentration gradients, the concept of an interface is still meaningful and well represented.

An initially circular ferrofluid droplet of diameter d and maximum central thickness of about 0.2 mm is placed on the bottom of a flat cavity, whose depth is 0.43 mm. The cavity is then filled with the nonmagnetic miscible fluid, so that the ferrofluid droplet is completely immersed in a thin layer of such a fluid. The magnetic fluid sample we use is a light mineral oil based commercially available ferrofluid (EMG901) produced by the Ferrotec Corporation. The viscosity and density of the ferrofluid are $\mu_d=10$ cP and $\rho d=1.53$ gm/ml, respectively. The surrounding nonmagnetic liquid is a particular type of mineral oil (carrier fluid of the ferrofluid EMG911 by Ferrotec Corp.) with $\mu_m=4$ cP and $\rho_m=0.89$ gm/ml. A uniform perpendicular magnetic field is provided by a pair of Helmholtz coils powered by programmable power suppliers. The power sources are turned on instantly to generate a uniform field strength of $H=755$ Oe and kept constant by fixing the current intensity. The time evolution of the diffusing interface separating the two miscible fluids is directly recorded from above by a charge-coupled device (CCD) camera, providing an upper view of

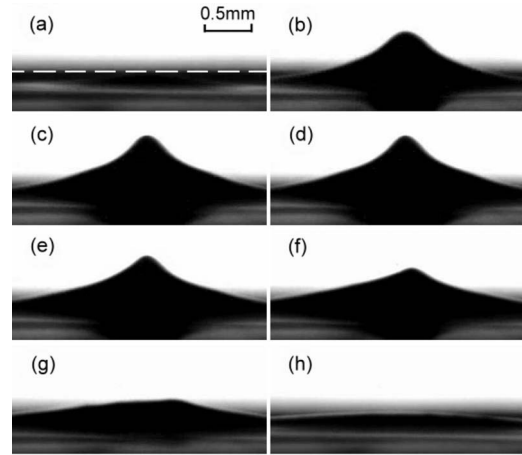


FIG. 2. Snapshots of side views at (a) $t=0$ s; (b) $t=0.2$ s; (c) $t=0.43$ s; (d) $t=0.5$ s; (e) $t=0.8$ s; (f) $t=1.2$ s; (g) $t=2.0$ s, and (h) $t=5.0$ s. The surface of the nonmagnetic solvent layer is identified by the horizontal white dashed line in (a).

the situation. Simultaneous side view images of the Rosensweig peak are conveniently taken via reflection from a prism. The two CCD cameras are connected to separate microscopes so that the pictures can be properly enlarged and recorded, and then transmitted to a computer.

Two kinds of experiments were run: (i) a free surface type flow, where a Rosensweig peak is allowed to emerge from the nonmagnetic fluid background and (ii) a confined fluid flow, where spatial confinement is imposed by placing a lid on the top of the fluid layer, aimed at studying the situation in which the Rosensweig peak formation is suppressed.

B. A decaying Rosensweig peak

Induced by the perpendicular magnetic field, a peculiar interfacial instability arises, which is a kind of hybrid type involving a modified Rosensweig instability in the direction perpendicular to the cavity, and a miscible labyrinthine-type instability occurring along the plane defined by the bottom of such a cavity. A representative case of an initially circular ferrofluid droplet of diameter $d=1.8$ mm is presented in Fig. 2 (side view) and Fig. 4 (top view) in order to elucidate the simultaneous occurrence of these two ferrohydrodynamic instabilities. The magnetic field is turned on at time $t=0$, when the ferrofluid surface is essentially flat, and parallel to the bottom of the cavity [Fig. 2(a)]. Similar to what happens in the conventional Rosensweig instability, at $t=0.2$ s the ferrofluid droplet is suddenly lifted by the perpendicular field, forming a typical vertical Rosensweig peak [Fig. 2(b)]. Note that this peak is in fact higher than the surface of the nonmagnetic solvent layer, which for clarity is identified by the horizontal white dashed line shown in Fig. 2(a). After that, the height of the peak beyond the surface fluid layer (denoted hereafter as h) keeps increasing, and reaches its maximum value ($h=0.546$ mm) at time $t=0.43$ s [Fig. 2(c)].

As time progresses, we observe a *sui generis* phenomenon which is completely absent in the conventional Rosensweig instability [6–8]. As illustrated in Figs. 2(d)–2(g), after reaching its maximum value, the height of the ferrofluid peak

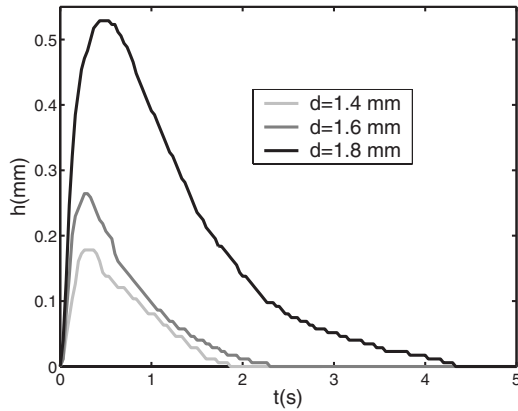


FIG. 3. Time evolution of the height of the miscible Rosensweig peak for three different values of the initial ferrofluid droplet diameter. The maximum peak heights are $h=0.178$ mm (for $d=1.4$ mm), $h=0.264$ mm (for $d=1.6$ mm), and $h=0.546$ mm (for $d=1.8$ mm). For each initial diameter, the reimmersing stage III begins at $t=1.9$ s (for $d=1.4$ mm), $t=2.3$ s (for $d=1.6$ mm), and $t=4.3$ s (for $d=1.8$ mm).

begins to decrease, and eventually the peak is completely reimmersed into the miscible surrounding layer of nonmagnetic fluid. This is in fact completely unlike the corresponding peak pattern formation in an immiscible ferrofluid: in the ordinary Rosensweig instability an equilibrium state is formed, being characterized by a ferrofluid peak with a well defined height. This steady peak is sustained by a balance between the net magnetic body force, gravity, and surface tension. However, for the miscible situation depicted in Fig. 2, transient diffusive effects occur at base region of the Rosensweig peak, where the ferrofluid is immersed in the miscible solvent fluid. Within this region the magnetic fluid diffuses into the surrounding nonmagnetic solvent. Consequently, the local magnetic force near the base of the peak is continuously weakened, and therefore unable to sustain a steady height against gravity. This is the reason why the height of the Rosensweig peak starts to diminish gradually, and nearly disappears as it reimmerses into the solvent fluid layer at $t=4.3$ s. A completely reimmersed peak is depicted in Fig. 2(h) at $t=5$ s.

On the basis of the experimental observations depicted in Fig. 2, we can identify three major stages characterizing the development of the Rosensweig peak instability under such miscible circumstances: first, we have the establishment of a rapidly growing stage I ($0 < t \leq 0.43$ s), followed by a longer decaying stage II ($0.43 < t < 4.3$ s), and finally, the occurrence of a reimmersing stage III ($t \geq 4.3$ s). We have verified that this three-stage description is considerably robust, and does not change if the diameter of the initially circular ferrofluid droplet is modified. This is clearly illustrated in Fig. 3 where the time evolution of the height of the Rosensweig peak is displayed for three increasing values of the initial droplet diameter d : 1.4 mm (light gray curve), 1.6 mm (dark gray curve), and 1.8 mm (black curve). It is clear that smaller droplets result in lower maximum peak heights, shorter time periods for stage II, and smaller reimmersing times (which indicate the beginning of stage III). In Fig. 3 notice that the curves for the 1.6 and 1.8 mm droplet diam-

eters appear to have similar shapes. Unfortunately, we have not been able to find a simple rescaling that would cause these curves to coincide. In addition, note that the shape of the curve for the 1.4 mm droplet differs from the other two, showing a more linear decay. We believe this might be due to the increased experimental inaccuracy related to measurements involving such a small droplet.

We emphasize that the very existence of the characteristic stages I, II, and III mentioned above is actually coupled to the simultaneous occurrence of an equally interesting interfacial phenomenon which takes place within the nonmagnetic fluid layer, and on the horizontal plane of the cavity. This is precisely a modified miscible version of the labyrinthine instability in magnetic fluids, which will be discussed in more detail in the remainder of this work.

As we have commented earlier, during the very short period of stage I, the growth of the Rosensweig peak mainly results from a three-dimensional force balance involving magnetic, gravitational, and surface tension effects. So, for stage I no significant flow on the horizontal plane of the cavity is expected. In contrast, the decay in the peak height occurring during stage II has important consequences with respect to the flow and pattern formation along the planar region at the bottom of the cavity. The decay phenomenon pushes the ferrofluid against the nonmagnetic fluid, and can be viewed as a sort of effective injection process which induces an outward radial flow on the horizontal plane of the cavity, leading to a ferrofluid droplet expansion. In a sense, this confined outward flow would be similar to the process of injecting a more viscous fluid against a less viscous one in a radial Hele-Shaw cell [24]. As for stage III, no significant additional radial flow is produced on the horizontal plane of the cavity, so that the resulting interfacial instability is predominantly determined by magnetic interactions.

It is worth pointing out that the formation of a single Rosensweig crest shown in Fig. 2 is significantly different from the recent experimental results obtained in Refs. [17,18]. As in our current problem, the authors in [17,18] study the behavior of a thin ferrofluid droplet under a perpendicular magnetic field configuration. However, they consider the immiscible situation in which the droplet is surrounded by air. In the immiscible case [17,18], the initial droplet is ruptured into numerous smaller droplets, each of them forming a new peak. This is very different from what is observed in Fig. 2, where the absence of surface tension leads to a smoother interfacial behavior, in which the droplet ruptures and multiple peak formation are not favored.

C. A different kind of labyrinthine instability

We now focus on the miscible labyrinthine instability which occurs on the plane of the cavity. Figure 4 shows the snapshots of the in-plane pattern formation process as the ferrofluid pushes the surrounding nonmagnetic liquid, as viewed from the top. The times taken in the upper views illustrated in Fig. 4 are the same as the ones used in the side view images shown in Fig. 2. In Fig. 4 the in-plane fluid flow can be seen as confined, or quasi-two-dimensional, due the capillary effects imposed by the free surface of the thin fluid

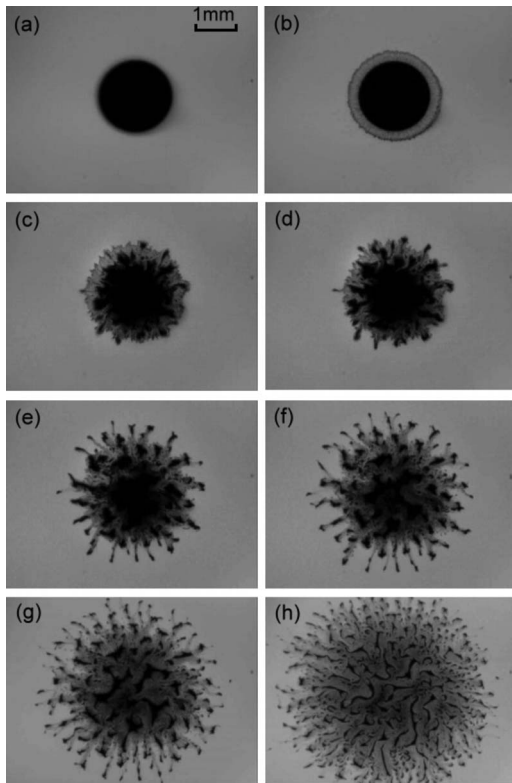


FIG. 4. Top views of the experiment shown in Fig. 2. The snapshot times in (a)–(h) are exactly the same as those used in Fig. 2. The initial circular shape shown in (a) has diameter $d=1.8$ mm.

layer of the nonmagnetic fluid. Within this spatially confined environment the applied magnetic field aligns the tiny magnetic moments of the ferrofluid along its direction. Consequently, these magnetic moments start to repel each other within the horizontal plane of the cavity, and the diffusing interface tends to deform.

According to the dynamical stages categorized in the discussion of Fig. 2, the upper view images shown in Figs. 4(a)–4(c), 4(d)–4(g), and 4(h) correspond to stages I, II, and III, respectively. As the magnetic field is applied at $t=0$ the border of the ferrofluid has an initially circular shape [Fig. 4(a)]. Right after this, the field causes a clear interfacial disturbance of the ferrofluid droplet. This sudden disturbance leads to the appearance of an annular mixing zone as shown in Fig. 4(b). The annular region arises as a consequence of the diffusion process that takes place when the ferrofluid peak emerges from the solvent layer. As described above, the dominant behavior during stage I is the rapid formation of the Rosensweig peak, so that the main body of the droplet as viewed from above preserves a nearly circular shape [Fig. 4(b)] having virtually the same area as the structure depicted in Fig. 4(a), without any significant morphological changes within it. As the peak reaches its maximum height, the mixing process around its base has already deposited a certain amount of magnetic fluid at the bottom of the cavity, so that in-plane magnetic repulsion starts to increase, leading to the formation of some fingering structures [Fig. 4(c)].

Nevertheless, once the evolution proceeds to stage II, when the miscible Rosensweig peak starts to decay, an in-

plane radially outward flow is induced, resulting in a slightly increased ferrofluid droplet area as shown in Fig. 4(d). Consequently, the formation of a more active fingering process can be indeed verified in Fig. 4(d). At first glance, the appearance of these slightly larger fingers seems to contradict the usual viscous fingering cliché that an interface should remain stable by the injection of a more viscous fluid into a less viscous one [24]. As a matter of fact, the more noticeable in-plane fingering in Fig. 4(d) arises due to a different mechanism, mainly related to the magnetic interactions within the ferrofluid. This can be qualitatively explained as follows: as the peak decays and the so-called “injection” process is initiated, an increasing amount of magnetic fluid is deposited in an effectively two-dimensional region within the nonmagnetic fluid solvent layer. Under such circumstances, the dipole-dipole magnetic repulsion becomes more intense so that the confined ferrofluid spreads out farther, and the mixing interface grows unstable. Therefore despite the viscosity-driven stable nature of such a continuous injection process, it favors the spatial confinement of the miscible magnetic fluid, which in turn triggers a labyrinthine-type instability.

As time advances, the cone-shaped Rosensweig crest keeps decaying, and the in-plane magnetic repulsion is intensified further, leading to even more active labyrinthine pattern formation as shown in Figs. 4(e)–4(g). During this stage II it is worth noting the occurrence of broken tentaclelike structures, where the finger tips tend to separate from the central body of the deforming interface. The occurrence of finger tip separations is connected to local thickness variations in the ferrofluid. Because of the accumulation of magnetic material in the cone-shaped surface along the vertical direction, the remaining flatter portions of the ferrofluid become significantly thinner far from the peak. As a result, slim and thinner fingers are easily pinched off by diffusion. In addition, as the peak decays, the convective transport induced by the in-plane radially outward injection further strengthens the finger tip brake up process. So, the in-plane area occupied by the ferrofluid pattern is continuously forming an increasingly flatter and thinner structure. This leads to more vigorous labyrinthine fingering by creating a longer contacting interface as illustrated by Figs. 4(f) and 4(g).

At later times, the miscible ferrofluid structures which have been fragmented into smaller pieces are stretched by strong magnetic repulsion effects, so that numerous bent slimmer fingers tend to appear. These structures have not been observed in previous labyrinthine formation experiments in confined ferrofluids [10,11,19,20]. Actually, the pattern depicted in Fig. 4(g) looks more similar in shape to the labyrinthine structures observed in growing grass in desert areas [13], and in drainage of granular-fluid systems [14]. Ultimately, after the complete reimmersion process of the Rosensweig peak, an interesting fragmented pattern is formed as shown in Fig. 4(h).

We close this section by stressing a very important point: notice that the miscible labyrinthine instability mechanism we propose in this work is markedly distinct from the one commonly used to describe the formation of labyrinthine patterns in Hele-Shaw cells with magnetic fluids [10,11,19,20]. Here the hybrid ferrohydrodynamic instability

arises due to a strong coupling between a diffusively induced 3D decaying process of a Rosensweig peak, and the simultaneous development of a quasi-2D fingering phenomenon resulting from the interplay between an in-plane injection process (induced by the peak decaying phenomenon) and a dipole-dipole magnetic repulsion within the ferrofluid.

D. A parallel between free surface and confined flow cases

In order to gain further insight about the unique features of the hybrid ferrohydrodynamic instability illustrated in Figs. 2 and 4, we introduce a small but important modification in our experimental setup and consider a confined miscible ferrofluid flow system. This is done by adding a lid on the top of the nonmagnetic fluid layer. The existence of such a lid prevents the formation of the 3D Rosensweig peak, and therefore some other type of confined miscible ferrofluid pattern is expected to be revealed. The experimental configuration we now propose is similar to the one used in recent studies of the miscible ferrofluid labyrinthine instability in Hele-Shaw cells [20,21]. However, in contrast to the practically 2D geometry of a Hele-Shaw setup, here the aspect ratio of the system ($d/b=1.8 \text{ mm}/0.43 \text{ mm} \sim 4.2$, where b represents the depth of the cavity) is too small, so that high aspect ratio [$\sim O(10-10^3)$], Darcy-law-type assumptions are not necessarily valid. The experimental results (upper view) for such a confined variation of our problem are depicted in Fig. 5, for the same times taken in the corresponding free surface experiments shown in Fig. 4. Therefore important features of the hybrid instability can be identified by comparing Figs. 4 and 5.

One evident difference is readily identified by contrasting Figs. 5(b) and 4(b): instead of producing an initially circular interface, the confined situation leads to considerably vigorous fingering right after the magnetic field is turned on. In addition, as opposed to the behavior illustrated in Figs. 4(c) and 4(d), mazelike fingering formation is very active already at early time stages in the confined system [Figs. 5(c) and 5(d)], tending to increase in intricacy as time progresses [Figs. 5(e) and 5(f)]. The way fingers arise and evolve under these two distinct conditions is actually very different: while in the confined situation fingering mainly occurs around the circumferential region of the droplet, in the unconfined case the fingers grow inside out, which leads to finger tip separations and favors a diffusive pinch-off phenomenon.

Although inward penetration of the outer nonmagnetic fluid is clearly observed in Figs. 5(g) and 5(h) in order to conserve mass, the inner droplet region remains fairly intact, so that finger break up and overall changes in droplet topology are contained. This is in flagrant contrast with what has been found in Figs. 4(g) and 4(h). Basically, despite the miscible nature of the confined flow in Fig. 5, the lack of a 3D peak decaying process accompanied by a quasi-2D injection mechanism is mainly responsible for allowing the development of intense fingering, however without the occurrence of the pinch-off events found in Fig. 4.

An additional point to be addressed is a morphological comparison between the confined patterns shown in Fig. 5, and the related structures obtained in equivalent Hele-Shaw

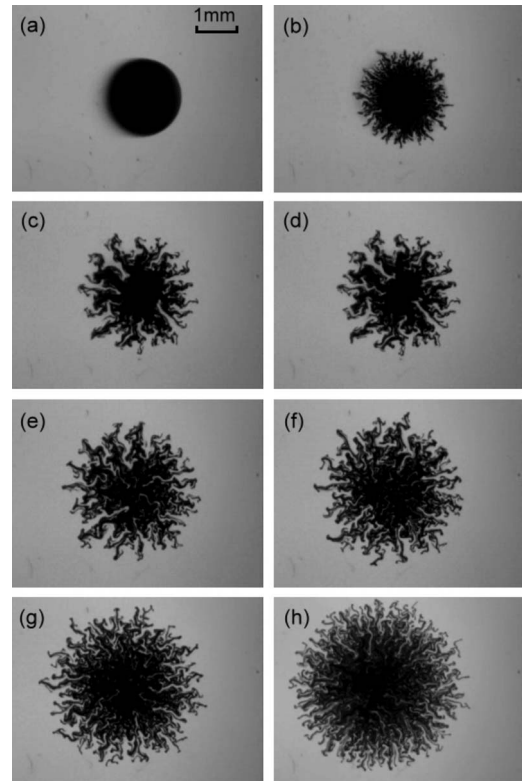


FIG. 5. Snapshots of the top views for the situation of a confined miscible ferrofluid droplet taken at the same times, and using the same physical parameters as those used in Fig. 4. The spatial confinement is provided by a lid located on the top the fluid layer which prevents the formation of the Rosensweig peak. The initial circular shape shown in (a) has diameter $d=1.8 \text{ mm}$.

cell experiments with miscible ferrofluids under a perpendicular magnetic field [20]. In Ref. [20] the droplet aspect ratio $d/b \sim 17-41$ (here b denotes the cell gap width) and very vigorous labyrinthine fingers are observed, which resemble greatly the ones depicted in Fig. 5. This close morphological similarity reinforces the significance of mostly 2D repelling magnetic forces in our current confined situation. On the other hand, the formation of secondary waves detected in Ref. [20], which are strongly affected by the cell gap width (wavelength $\lambda \approx 7b$), are completely absent in the pattern formation process illustrated in Fig. 5. The absence of such secondary waves can be attributed to the small aspect ratio of the present confined case, where $d/b \sim 4.2$. Considering the equivalent gap width (the depth of cavity) $b = 0.43 \text{ mm}$ for the confined case in Fig. 5, the wavelength of the secondary waves would be roughly given by $\lambda \approx 3 \text{ mm}$. For a droplet of diameter $d=1.8 \text{ mm}$ as the one in Fig. 5, it would not be possible to accommodate the formation of a multinode of such secondary waves. So, our present experiment also provides an indirect verification that the existence of these secondary waves [20] are predominantly determined by 3D effects.

An alternative and more quantitative account of the main differences between the free surface (or, unconfined) flow shown in Fig. 4, and the confined flow depicted in Fig. 5 is provided in Fig. 6. The images of both experiments are first

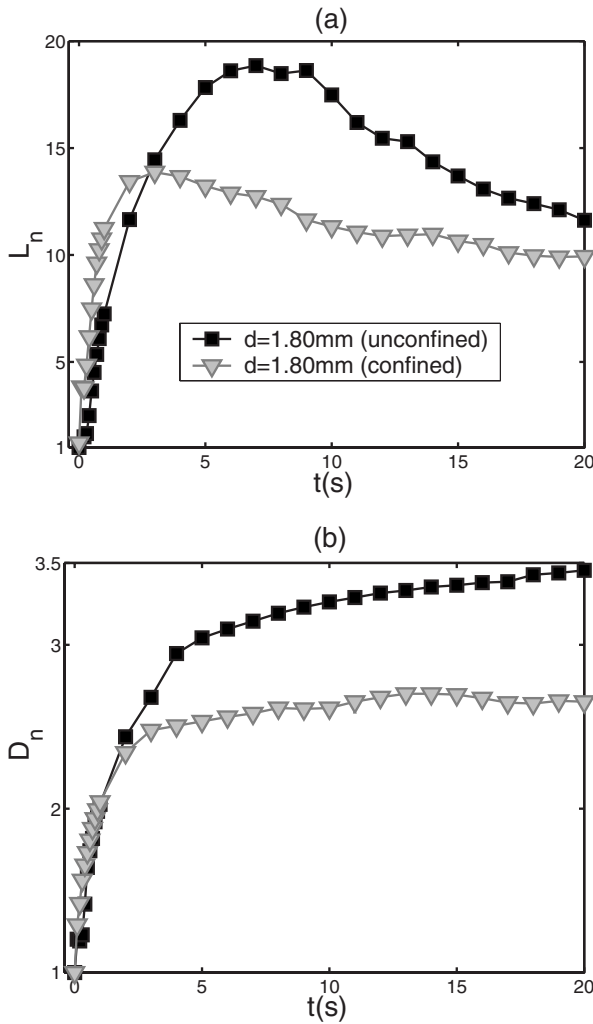


FIG. 6. Normalized mixing interfacial length L_n (a), and normalized diameter of gyration D_n (b) plotted as a function of time, for the case of the free surface (unconfined) experiment shown in Fig. 4 (back squares) and its confined counterpart depicted in Fig. 5 (gray triangles).

scanned into a MATLAB software to measure the correspondent hue values of the entire pattern forming domain S . With the processed scanned images of the experiments at hand, two useful characteristic quantities [23,25] can be computed: (i) the normalized mixing interfacial length

$$L_n = \frac{L(t)}{L(t=0)},$$

where

$$L(t) = \int_S \sqrt{\left(\frac{\partial c}{\partial x}\right)^2 + \left(\frac{\partial c}{\partial y}\right)^2} dx dy,$$

and c is the concentration of the ferrofluid approximated by hue values; and (ii) the normalized diameter of gyration $D_n = D_g(t)/D_g(t=0)$, where D_g is the longest distance between two nonmagnetic fluid elements diffusively invaded by the miscible ferrofluid in the scanned images. Alternatively, we can say that D_n is a measure of the size of the ferrofluid spot

at a given time. Figure 6 illustrates how the dimensionless quantities (a) L_n and (b) D_n vary with time ($0 \leq t \leq 20$ s), for the unconfined (back squares) and confined (gray triangles) experiments shown in Figs. 4 and 5, respectively.

For the unconfined case in Fig. 6(a), we see a rapid initial growth for L_n , before a sort of “plateau” is established for $5 < t < 10$ s, followed by a decaying behavior for $t > 10$ s. Since the dynamical stage I defined earlier in this work is too short to show significant changes in Fig. 6(a), we begin by focusing what happens after its occurrence. In agreement with the results obtained in Refs. [23,25], the rapid growth of L_n up until $t=5$ s indicates an increasing interfacial instability. Here such an instability is induced by the injectionlike process which takes place at stage II. After that, even though no obvious injection is present to favor enhanced fingering, the interfacial length is sustained by the significant magnetic repulsion effects still existing at the beginning of stage III ($5 < t < 10$ s). Nevertheless, strong diffusion eventually overcomes such magnetic effects, and the interfacial length starts to drop after $t > 10$ s.

This free surface flow scenario is modified for the equivalent confined situation (gray triangles) in Fig. 6(a). Although the confined patterns in Fig. 5 are very convoluted, fingering is mainly triggered at the circumferential region of the diffusing interface. Moreover, any sort of interfacial break up is clearly restrained. As a result, the growing time period of L_n for the confined flow (time until reaching a maximum) is shorter than that for its free surface analog. On the other hand, the time growth rate of L_n for the confined case (given by the slope of the gray curve) is higher, in line with the fact that labyrinthine fingering arises shortly after the magnetic field is applied. Due to the lack of an auxiliary injection mechanism in the confined case, after reaching a maximum the curve representing L_n drops off as time advances, lying always below the black curve associated to the unconfined flow behavior.

Now we turn to the analysis of the time evolution of the normalized diameter of gyration as plotted in Fig. 6(b). Roughly speaking, D_n can be seen as a measure for the efficiency of the mixing, or as an indicator for the tendency toward interfacial break up and morphological disintegration of the initial pattern into smaller portions. For the unconfined situation, we observe a rapid increase of D_n up until $t=5$ s (stage II). This is exactly the time interval during which the Rosensweig peak decays, so that the in-plane injection mechanism favors active finger tip separation and pinch-off events. Following this, the droplet expansion is mainly dominated by magnetic effects and diffusion (instead of injection), and the growth of the gyration diameter slows down significantly for $t > 5$ s (stage III) tending to a saturation for larger times. On the other hand, initially the confined flow case also reveals an equally intense, but shorter period of growth for D_n . After reaching a maximum, we see that D_n does not change much with time, with the gray curve lying below the black one. Here the quick initial growth is mostly induced by strong repulsive magnetic effects within the ferrofluid. However, without the help of an induced injection process in the confined case, the diameter of gyration stabilizes, meaning that mixing is not as efficient as in the unconfined case.

III. CONCLUDING REMARKS

Our experimental results make evident that the proper interplay between the Rosensweig peak formation and the miscible nature of the fluids involved, in conjunction with the small thickness of the miscible ferrofluid sample, leads to a hybrid type of ferrohydrodynamic instability which unveils a variety of interesting dynamic phenomena plus a wealth of pattern forming behaviors. From our observations, many physical processes seem to influence the pattern formation mechanism in our system: diffusion, flow, convection, and magnetic effects. However, the most distinguished aspect of our study is that the pattern formation process in one direction (rising and decaying of the miscible Rosensweig peak in the perpendicular direction to the cavity) is indeed nontrivially coupled to a different pattern-forming phenomenon which simultaneously occurs along another direction (miscible labyrinthine-type instability along the plane of the cavity). In conclusion, in contrast to usual pattern formation studies performed in ferrofluids to date, we have discovered a different kind of ferrohydrodynamic instability that forms almost 2D labyrinth patterns and fully 3D ferrofluid peaked structures at the same time, in a single (relatively simple) experiment.

Of course, much remains to be done to reach a more quantitative understanding of this complex ferrohydrodynamic problem. It would be of interest to see whether the patterned structures we have found could be explained through more quantitative theoretical descriptions, and also appropriately modeled by accurate numerical simulations. The suggestive cooperative behavior between the 3D peak decaying process, and the effectively 2D growth of the ferrofluid droplet reveals a profusion of still unexplained interesting physics which we believe warrants further investigation. Despite the evident challenging nature of such theoretical enterprise, we hope this will be a subject of future research by investigators within the pattern formation and fluid mechanics communities.

ACKNOWLEDGMENTS

J.A.M. thanks CNPq (Brazilian Research Council) for financial support of this research through the program “Instituto do Milênio de Fluidos Complexos” Contract No. 420082/2005-0, and also through the CNPq/FAPESQ Pronex program. C.-Y.C. thanks the National Science Council of the Republic of China for financial support of this research through Grant No. NSC 96-2221-E-009-244-MY3.

-
- [1] R. E. Rosensweig, *Ferrohydrodynamics* (Cambridge University Press, Cambridge, England, 1985).
- [2] E. Blums, A. Cebers, and M. M. Maiorov, *Magnetic Fluids* (de Gruyter, New York, 1997).
- [3] B. M. Berkovski and V. Bashtovoy, *Magnetic Fluids and Applications Handbook* (Begell House, New York, 1996).
- [4] J.-C. Bacri, R. Perzynski, and D. Salin, *Endeavour* **12**, 76 (1988).
- [5] C. Rinaldi, A. Chaves, S. Elborai, X. He, and M. Zahn, *Curr. Opin. Colloid Interface Sci.* **10**, 141 (2005).
- [6] M. D. Cowley and R. E. Rosensweig, *J. Fluid Mech.* **30**, 671 (1967).
- [7] R. Friedrichs and A. Engel, *Phys. Rev. E* **64**, 021406 (2001).
- [8] R. Richter and I. V. Barashenkov, *Phys. Rev. Lett.* **94**, 184503 (2005).
- [9] G. I. Taylor, *Proc. R. Soc. London, Ser. A* **280**, 383 (1964).
- [10] A. O. Tsebers and M. M. Maiorov, *Magnetohydrodynamics (N.Y.)* **16**, 21 (1980).
- [11] D. P. Jackson, R. E. Goldstein, and A. O. Cebers, *Phys. Rev. E* **50**, 298 (1994).
- [12] R. E. Rosensweig, M. Zahn, and R. Shumovich, *J. Magn. Mater.* **39**, 127 (1983).
- [13] J. von Hardenberg, E. Meron, M. Shachak, and Y. Zarmi, *Phys. Rev. Lett.* **87**, 198101 (2001).
- [14] B. Sandnes, H. A. Knudsen, K. J. Måløy, and E. G. Flekkøy, *Phys. Rev. Lett.* **99**, 038001 (2007).
- [15] B. M. Berkovsky and V. Bashtovoi, *IEEE Trans. Magn.* **16**, 288 (1980).
- [16] J.-C. Bacri, R. Perzynski, and D. Salin, *C. R. Acad. Sci., Ser. II: Mec., Phys., Chim., Sci. Terre Univers* **307**, 669 (1988).
- [17] C.-Y. Chen and L.-W. Lo, *J. Magn. Magn. Mater.* **305**, 440 (2006).
- [18] C.-Y. Chen, C.-H. Chen, and L.-W. Lo, *J. Magn. Magn. Mater.* **310**, 2832 (2007).
- [19] M. M. Maiorov and A. O. Tsebers, *Magnetohydrodynamics (N.Y.)* **19**, 376 (1983).
- [20] C.-Y. Wen, C.-Y. Chen, and D.-C. Kuan, *Phys. Fluids* **19**, 084101 (2007).
- [21] C.-Y. Chen, *Phys. Fluids* **15**, 1086 (2003).
- [22] M. Igonin and A. Cebers, *Phys. Fluids* **15**, 1734 (2003).
- [23] C.-Y. Chen, S.-Y. Wu, and J. A. Miranda, *Phys. Rev. E* **75**, 036310 (2007).
- [24] L. Paterson, *J. Fluid Mech.* **113**, 513 (1981).
- [25] C.-Y. Chen, C.-H. Chen, and J. A. Miranda, *Phys. Rev. E* **71**, 056304 (2005).